

Supplementary Information

Highly porous copper-supported magnetic nanocatalyst: Made of volcanic pumice textured by cellulose, applied for reduction of nitrobenzene derivatives

Reza Taheri-Ledari¹, Mahdi Saeidirad¹, Fateme Sadat Qazi¹, Atefeh Fazeli¹, Ali Maleki^{*,1}, Ahmed Esmail Shalan^{*,2,3,+}


¹ *Catalysts and Organic Synthesis Research Laboratory, Department of Chemistry, Iran University of Science and Technology (IUST), Tehran 16846-13114, Iran.*

² *BCMaterials, Basque Center for Materials, Applications and Nanostructures, Martina Casiano, UPV/EHU Science Park, Barrio Sarriena s/n, Leioa 48940, Spain.*

³ *Central Metallurgical Research and Development Institute (CMRDI), P.O. Box 87, Helwan, Cairo 11421, Egypt.*

**Corresponding authors. (A. M) Tel.: +98 21 77240640-50; fax: +98 21 73021584. E-mail address: maleki@iust.ac.ir; (A. E. S.) E-mail: ahmed.shalan@bcmaterials.net; a.shalan133@gmail.com*

+ Currently on leave from CMRDI.

 *Author's ORCIDs:*

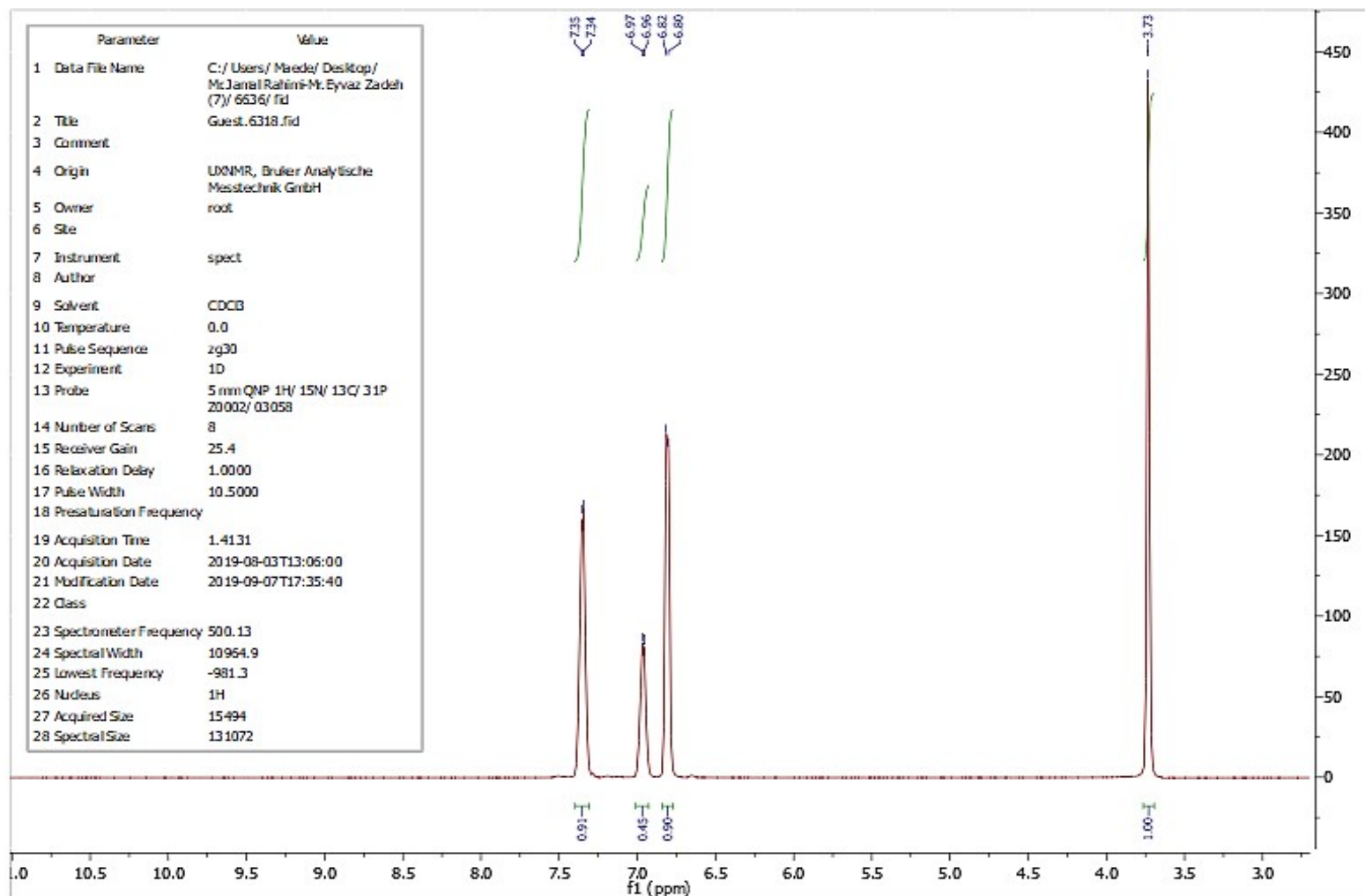
Reza Taheri-Ledari: <https://orcid.org/0000-0002-6511-9411>

Ali Maleki: <https://orcid.org/0000-0001-5490-3350>

Ahmed Esmail Shalan: <https://orcid.org/0000-0002-3424-1609>

Table of content

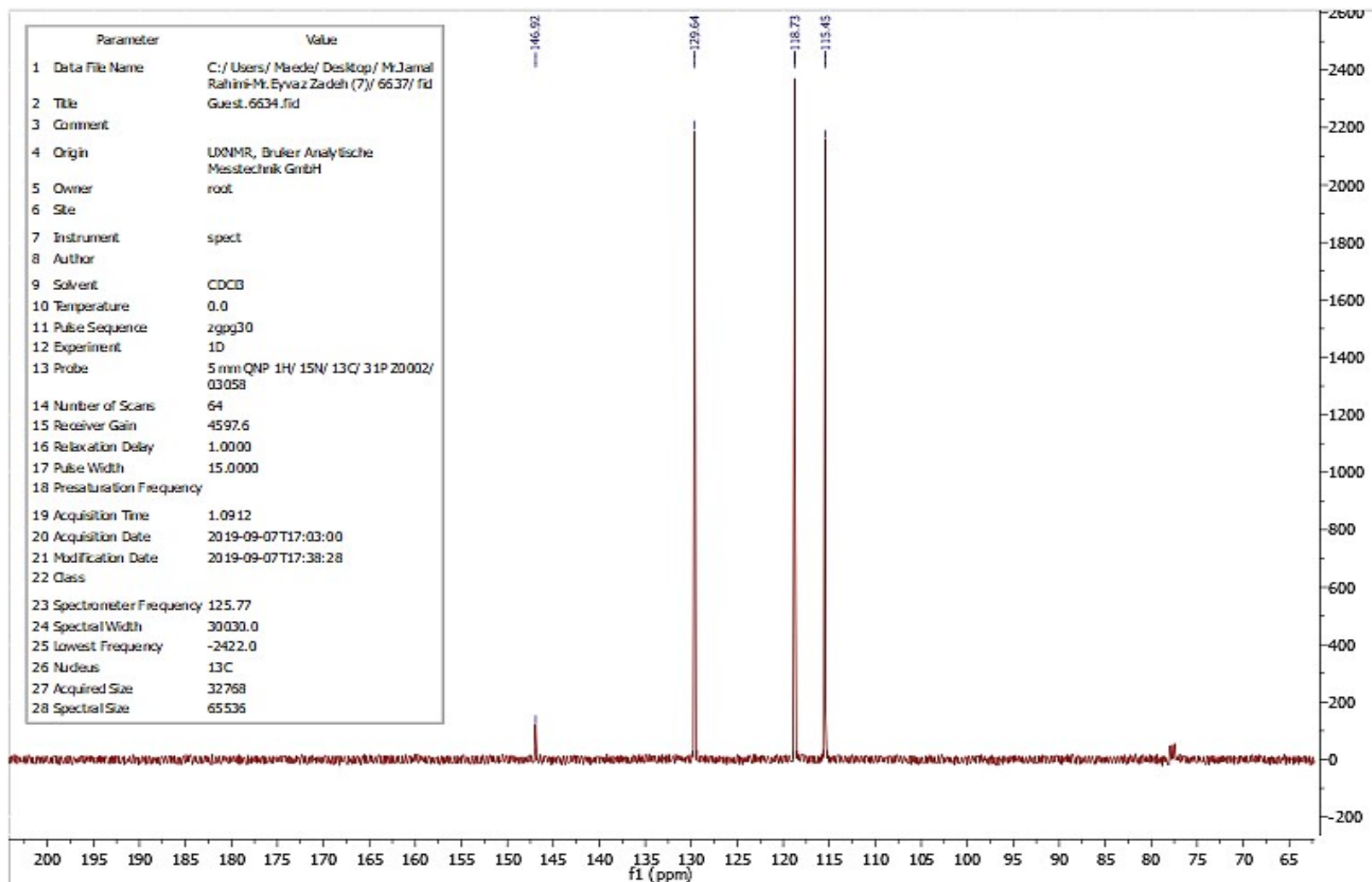
Content	Page
Figure S1. ¹ H-NMR spectra and spectral data of aniline	S3
Figure S2. ¹³ C-NMR spectra and spectral data of aniline	S4
Figure S3. ¹ H-NMR spectra and spectral data of benzene-1,4-diamine	S5
Figure S4. ¹³ C-NMR spectra and spectral data of benzene-1,4-diamine	S6
Figure S5. ¹ H-NMR spectra and spectral data of 2-amino-4-chloro-phenol	S7
Figure S6. ¹³ C-NMR spectra and spectral data of 2-amino-4-chloro-phenol	S8
Figure S7. ¹ H-NMR spectra and spectral data of 2-aminophenol	S9
Figure S8. ¹³ C-NMR spectra and spectral data of 2-aminophenol	S10
Figure S9. ¹ H-NMR spectra and spectral data of 4-amino-benzonic acid	S11
Figure S10. ¹³ C-NMR spectra and spectral data of 4-amino-benzonic acid	S12
Figure S11. ¹ H-NMR spectra and spectral data of 4-amino-phenol	S13
Figure S12. ¹³ C-NMR spectra and spectral data of 4-amino-phenol	S14
Figure S13. ¹ H-NMR spectra and spectral data of benzene-1,3-diamine	S15
Figure S14. ¹³ C-NMR spectra and spectral data of benzene-1,3-diamine	S16
Figure S15. ¹ H-NMR spectra and spectral data of 2-Naphthylamine	S17
Figure S16. ¹³ C-NMR spectra and spectral data of 2-Naphthylamine	S18
Figure S17. ¹ H-NMR spectra and spectral data of p-toluidine	S19
Figure S18. ¹³ C-NMR spectra and spectral data of p-toluidine	S20
Figure S19. ¹ H-NMR spectra and spectral data of 4-chloroaniline	S21
Figure S20. ¹³ C-NMR spectra and spectral data of 4-chloroaniline	S22
Table S1. Results of ICP-OES analysis of Fe ₃ O ₄ @VPMP/CLS-Cu nanocomposite	S23
Estimation of the catalyst amount in mmol% based on ICP-OES results	S23
Calculation of turnover number (TON) and turnover frequency (TOF)	S24
Estimation of half-life of the reduction reaction of nitrobenzene and investigation of reusability of Fe ₃ O ₄ @VPMP/CLS-Cu catalytic system	S25
Figure S21. Calibration curves of nitrobenzene, and (b) UV-Vis absorbance spectra of the NB reaction mixture, under catalytic conditions in different times	S25
Table S2. The yields and half-life values obtained for the reduction reaction of nitrobenzene (NB), under catalytic conditions provided by Fe ₃ O ₄ @VPMP/CLS-Cu system during five times reuse	S26
Table S3. Results of ICP-MS analysis on copper ion exist in supernatants after separation of the magnetic particles, after running each recycling process (leaching test)	S26
Table S4. Results of ICP-OES analysis of the recovered Fe ₃ O ₄ @VPMP/CLS-Cu nanocomposite.	S27
Figure S22. The graph of the optimization stages of reduction reaction of nitrobenzene under various catalytic conditions (related to Table 1).	S28



1. Aniline (Table 2 – Entry 1)

^1H NMR (500 MHz, CDCl_3): δ 3.73 (s, 2 H), 6.80-6.82 (d, J = 10 Hz, 2 H), 6.93-6.99(m, 1H), 7.34-7.35 (d, J = 5 Hz, 2 H).

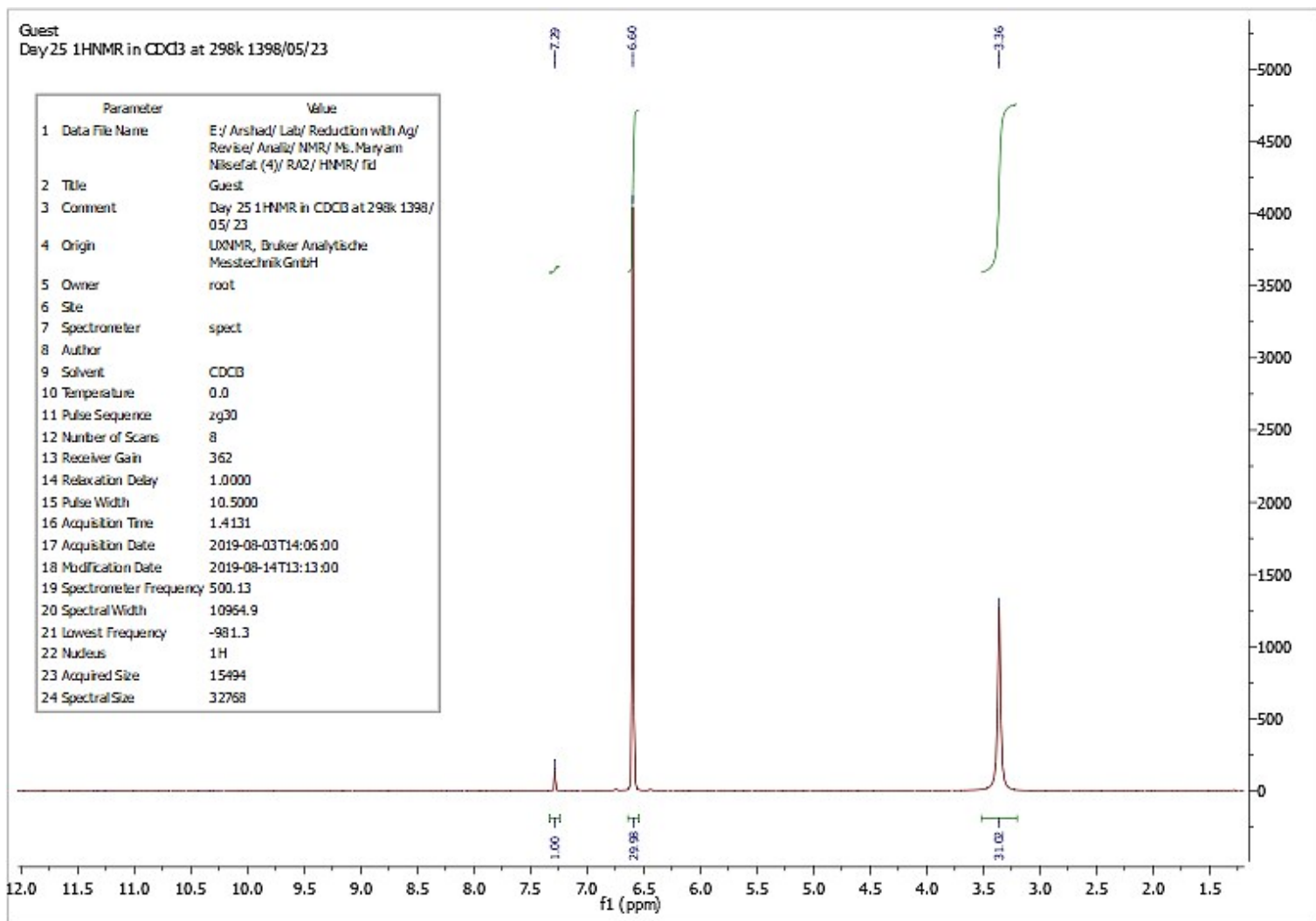
Figure S1. ^1H -NMR spectrum and spectral data of aniline.



1. Aniline (Table 2 – Entry 1)

^{13}C NMR (500 MHz, CDCl_3): δ 146.92, 129.64, 118.73, 115.45.

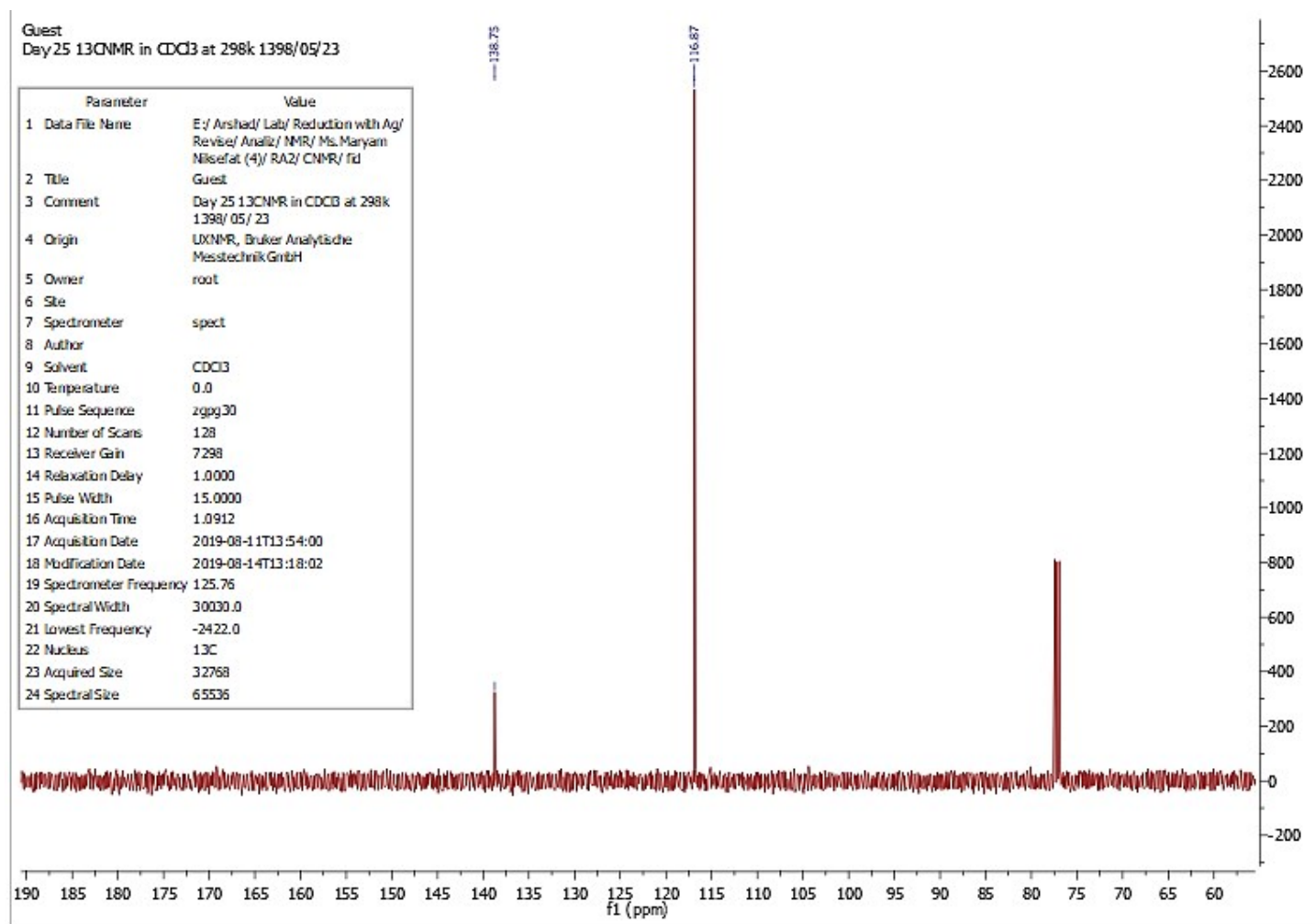
Figure S2. ^{13}C NMR spectrum and spectral data of aniline.



2. benzene-1,4-diamine (**Table 2 – Entry 2**)

¹H NMR (500 MHz, CDCl₃): δ 6.59 (s, 4 H), 3.36 (s, 4 H).

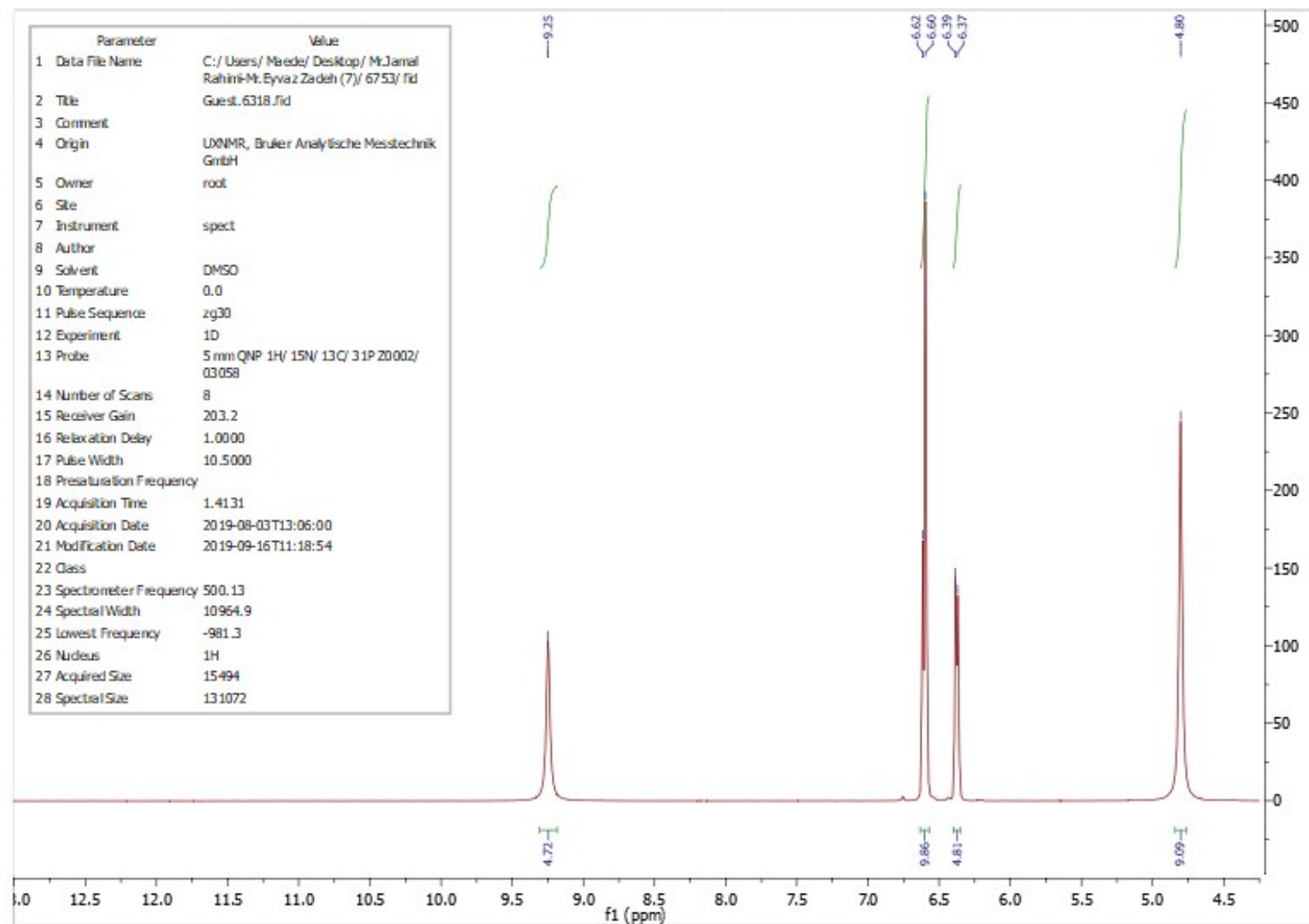
Figure S3. ¹H-NMR spectrum and spectral data of benzene-1,4-diamine.



2. benzene-1,4-diamine (Table2 – Entry 2)

^{13}C NMR (500 MHz, CDCl_3): δ 138.75, 116.87.

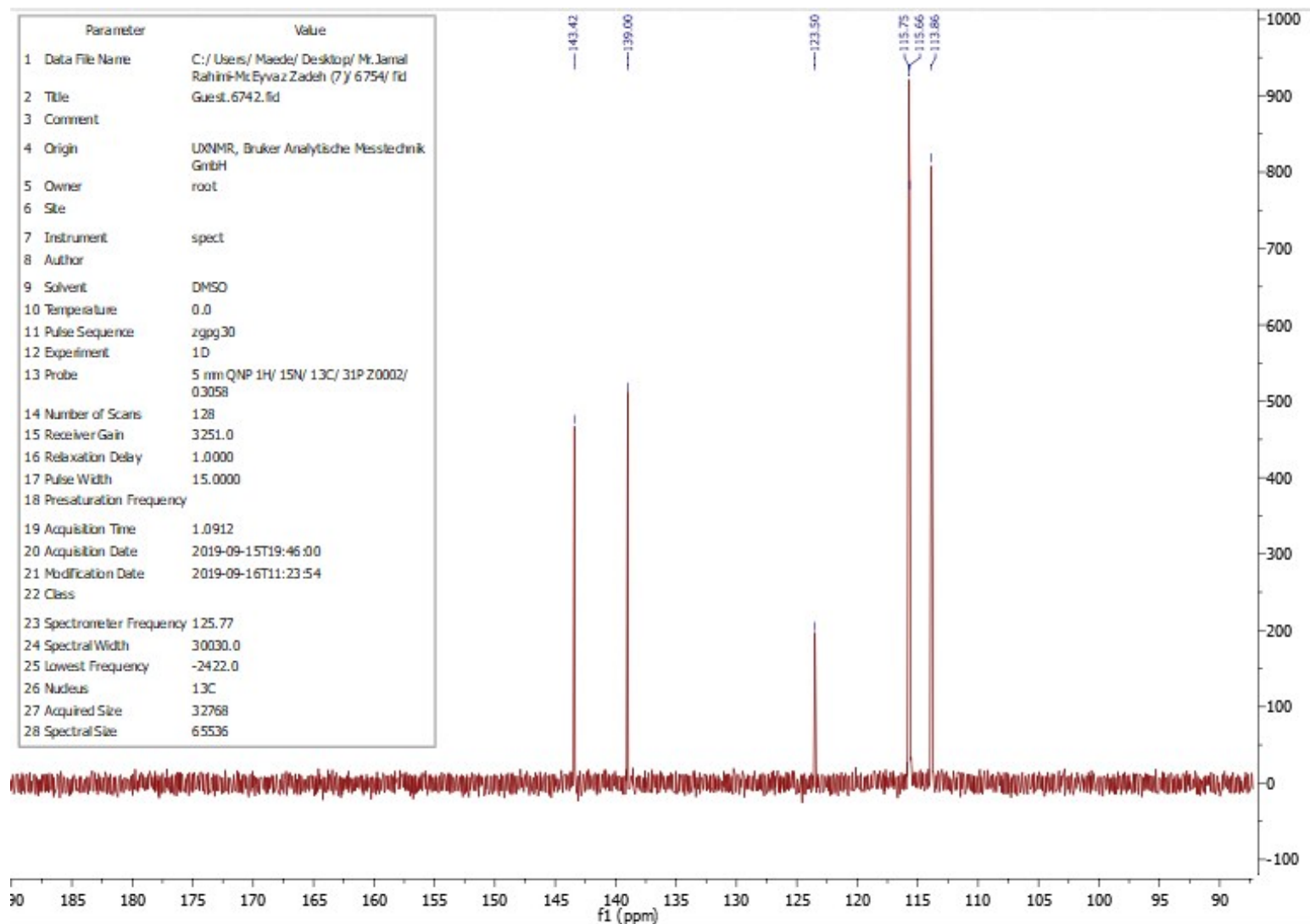
Figure S4. ^{13}C -NMR spectra and spectral data of benzene-1,4-diamine.



3. 2-amino-4-chloro-phenol (Table 2 – Entry 3)

^1H NMR (500 MHz, DMSO): δ 9.25 (s, 1H), 6.61 (m, 1H), 6.61 (m, 1H), 6.38 (m, 1H), 4.80 (s, 2H).

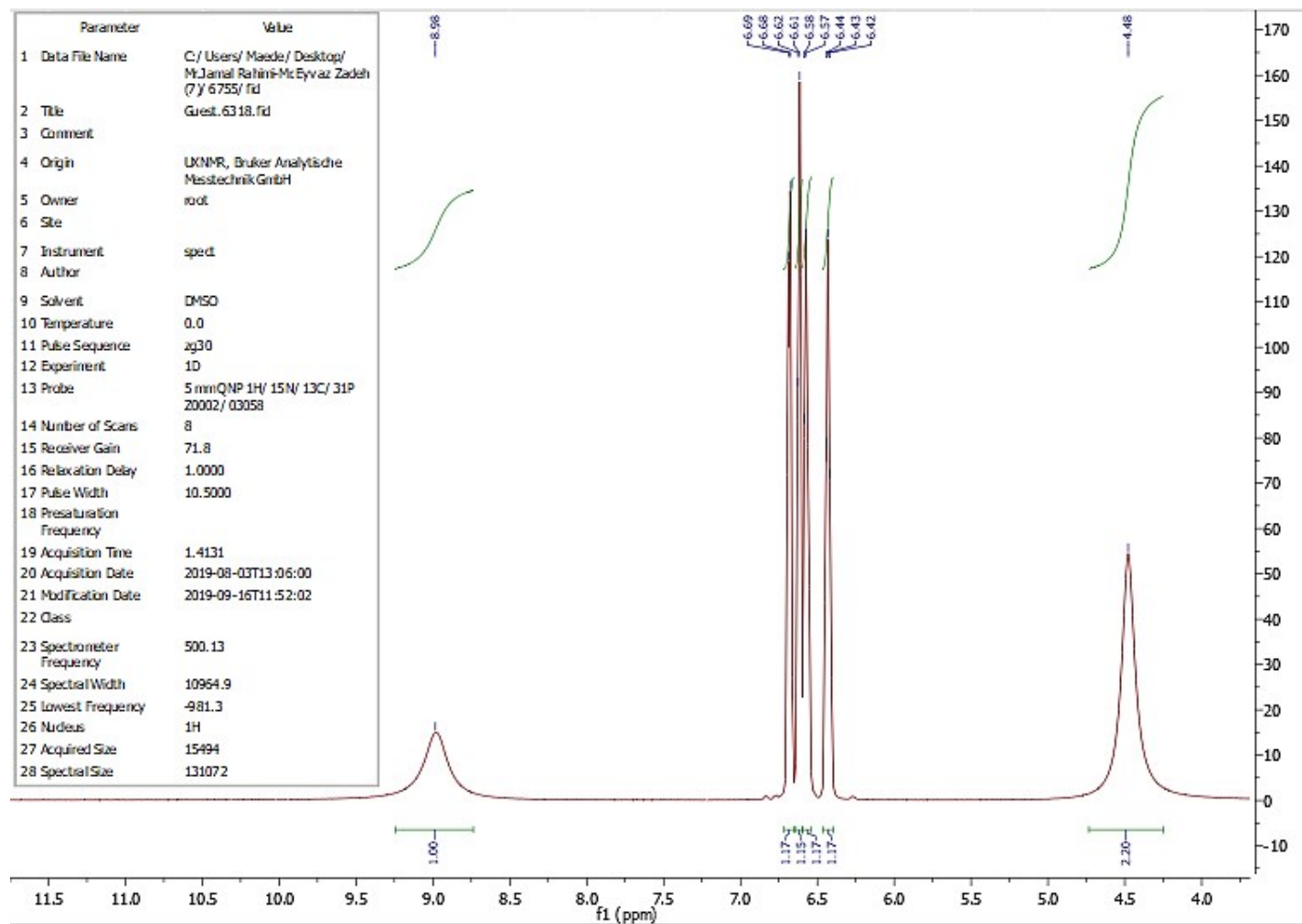
Figure S5. ^1H -NMR spectra and spectral data of 2-amino-4-chloro-phenol.



3. 2-amino-4-chloro-phenol (Table 2 – Entry 3)

^{13}C NMR (500 MHz, DMSO): δ 143.42, 139.00, 123.50, 115.75, 115.66, 113.86.

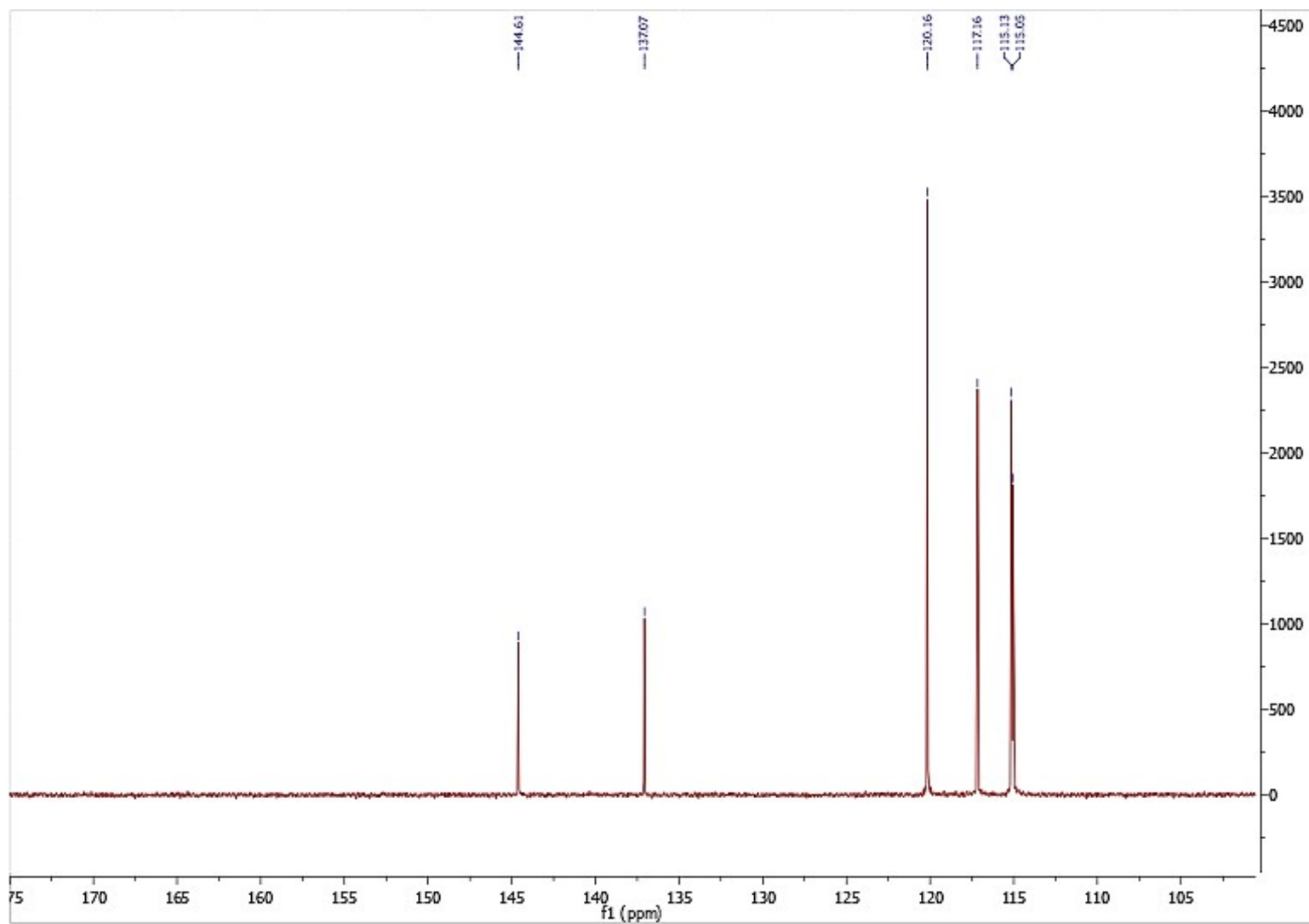
Figure S6. ^{13}C -NMR spectra and spectral data of 2-amino-4-chloro-phenol.



4. 2-aminophenol (Table 2 – Entry 4)

^1H NMR (500 MHz, DMSO): δ 8.98 (s, 1H), 6.68 (m, 1H), 6.61 (m, 1H), 6.57 (m, 1H), 6.43 (m, 1H), 4.48 (S, 2H).

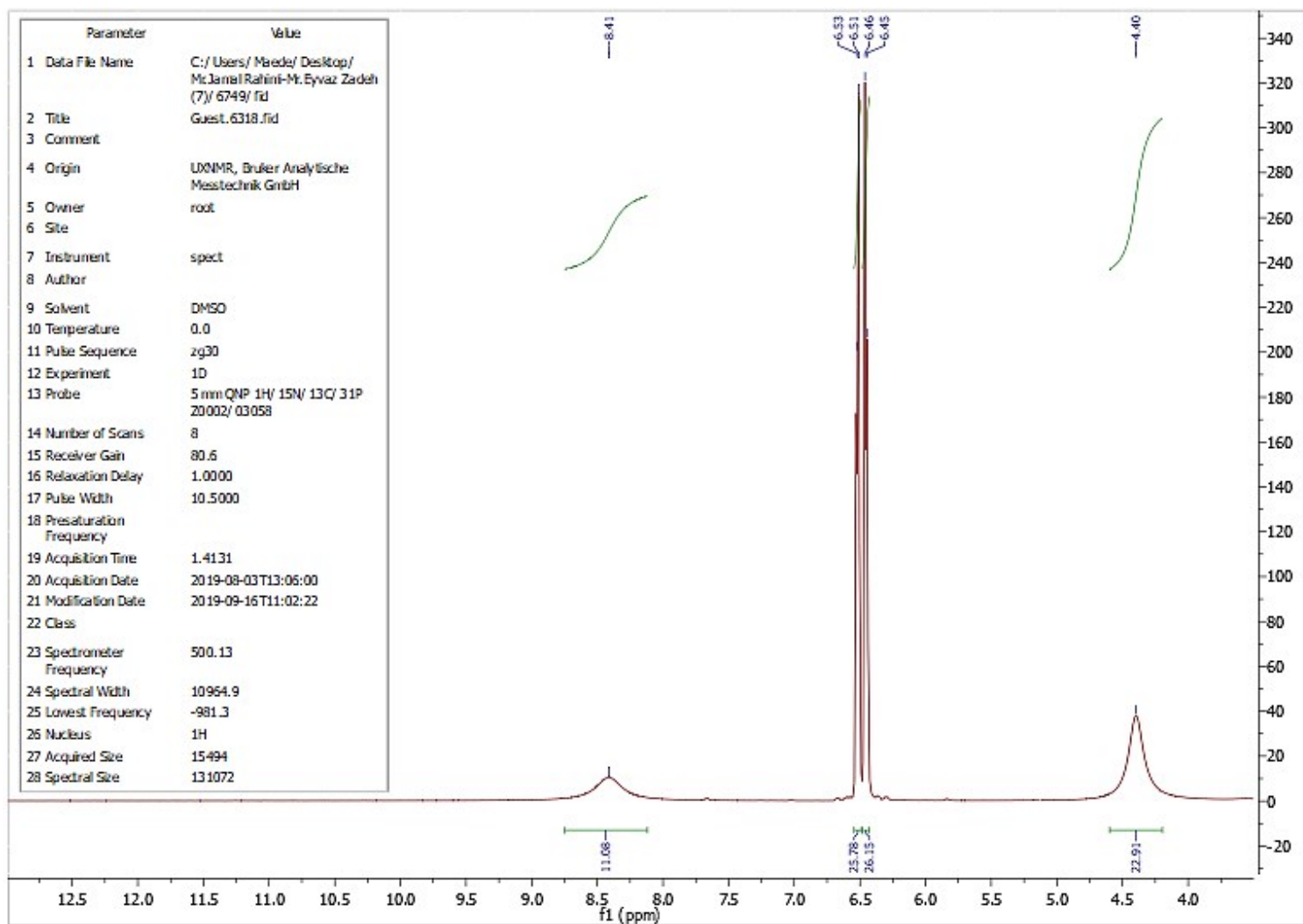
Figure S7. ^1H -NMR spectra and spectral data of 2-aminophenol.



4. 2-aminophenol (Table 2 – Entry 4)

¹³C NMR (500 MHz, DMSO): δ 144.51, 137.07, 120.16, 117.16, 115.13, 115.05.

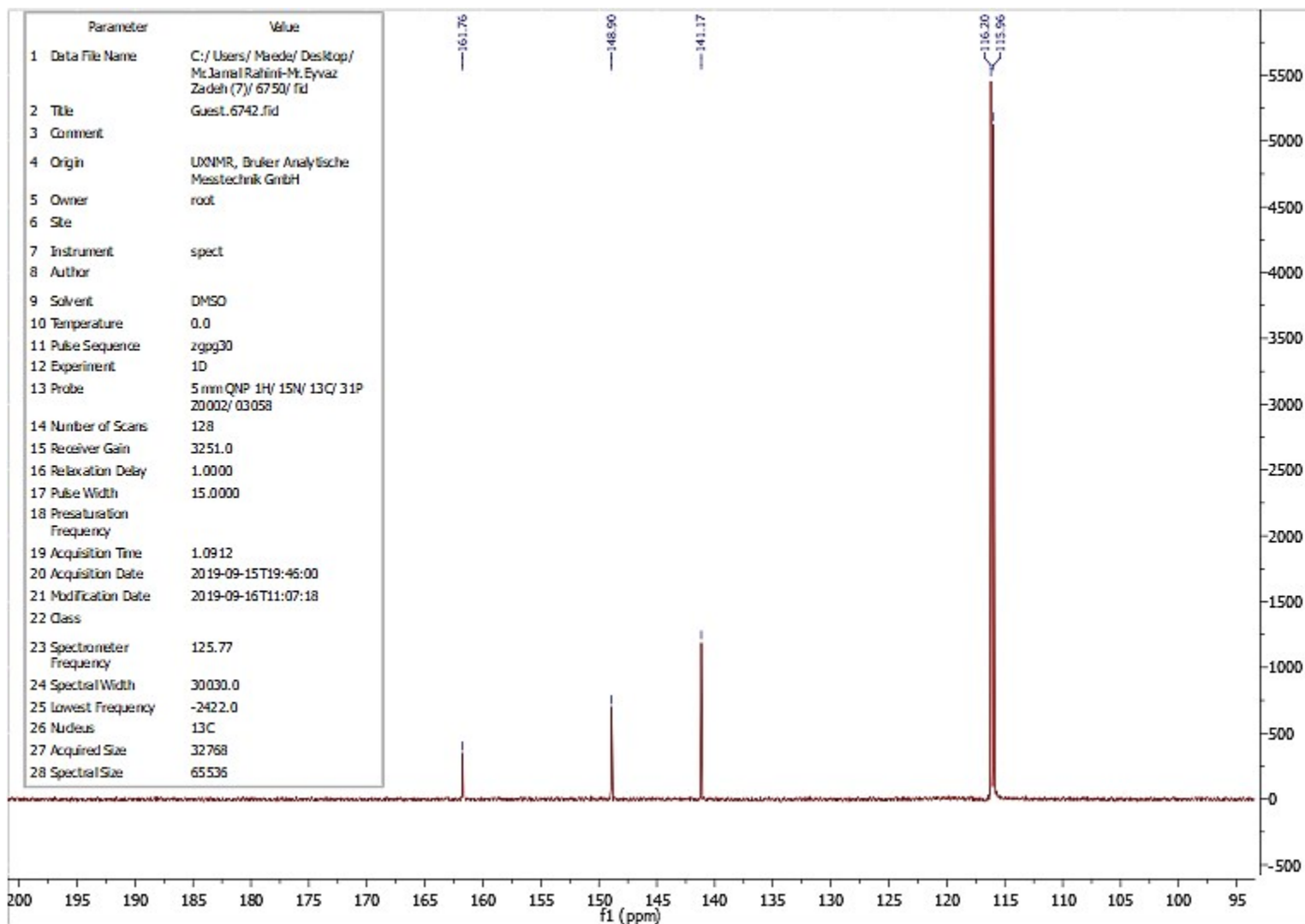
Figure S8. ¹³C-NMR spectra and spectral data of 2-aminophenol.



5. 4-amino-benzonic acid (Table 2 – Entry 5)

¹H NMR (500 MHz, DMSO): δ 8.41 (s, 1H), 6.53-6.51 (d, J = 10 Hz, 2H), 6.46-6.45 (d, J = 5 Hz, 2H), 4.40 (s, 2H).

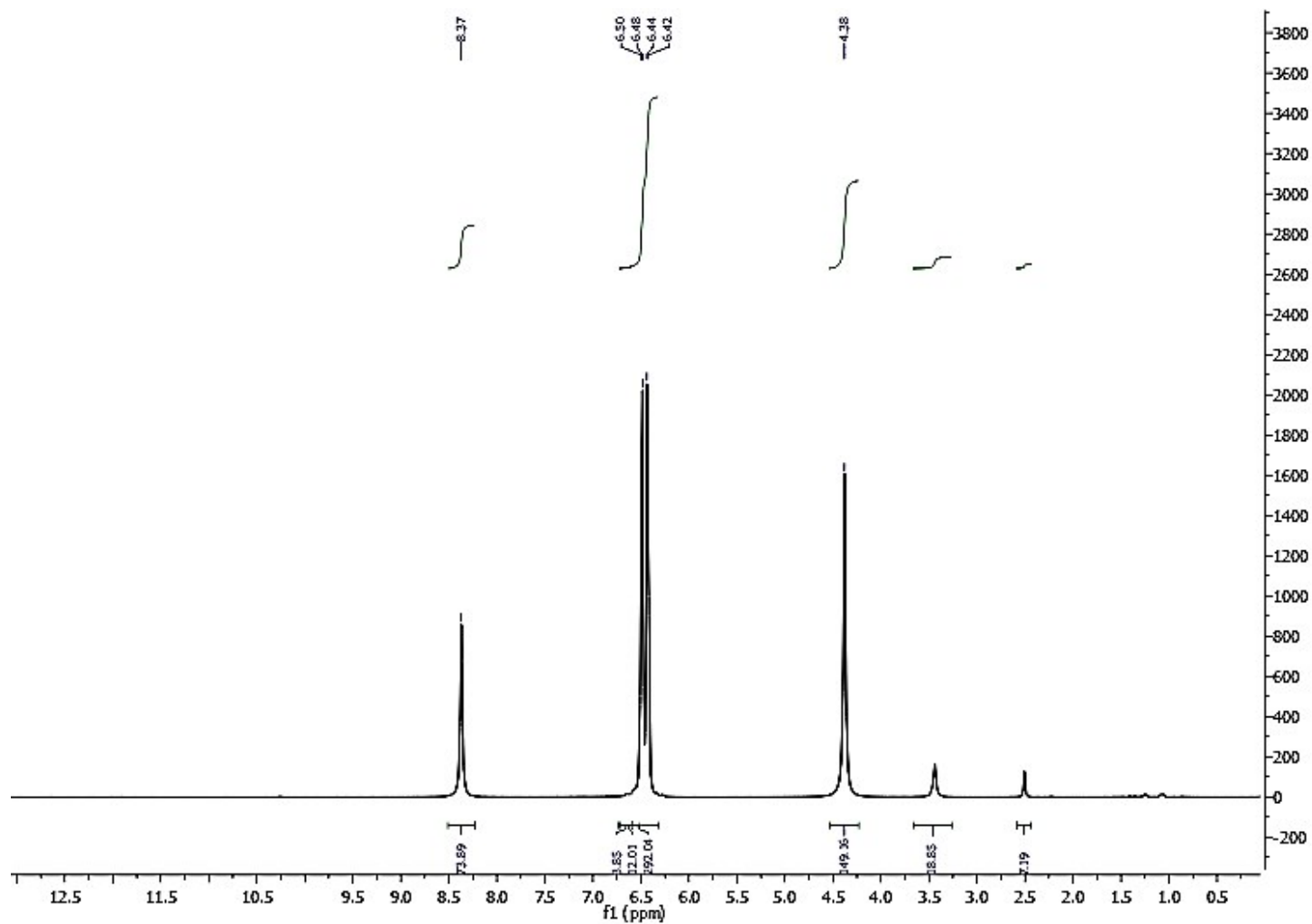
Figure S9. ¹H-NMR spectra and spectral data of 4-amino-benzonic acid.



5. 4-amino-benzonic acid (Table 2 – Entry 5)

^{13}C NMR (500 MHz, DMSO): δ 161.76, 148.90, 141.17, 116.20, 115.96.

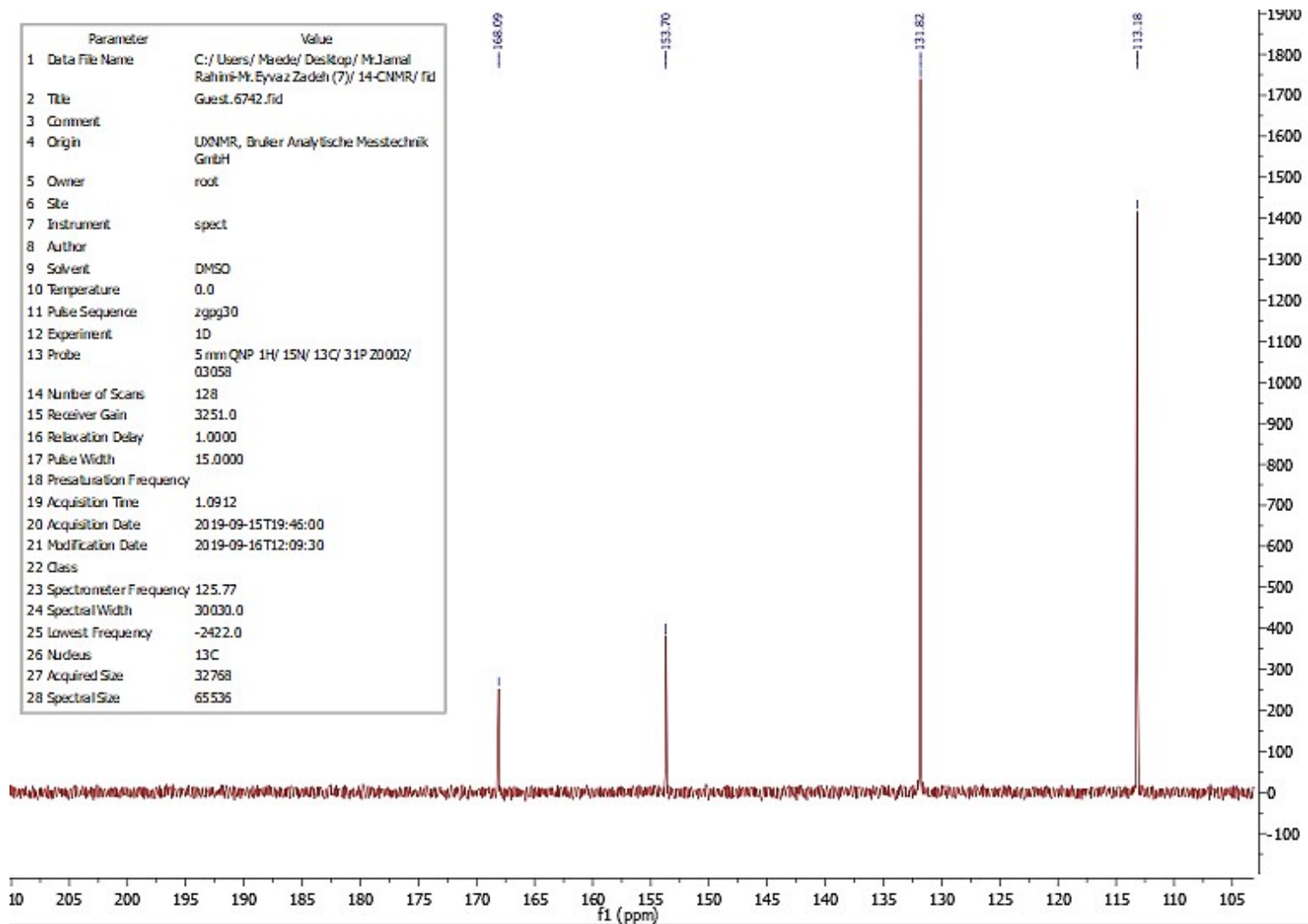
Figure S10. ^{13}C -NMR spectra and spectral data of 4-amino-benzonic acid.



6. 4-amino-phenol (Table 2 – Entry 6)

¹H NMR (500 MHz, DMSO): δ (ppm) = 4.38 (2H, s, NH₂), 6.42–6.44 (2H, d, J=10 Hz, H–Ar), 6.48–6.50 (2H, d, J=10 Hz, H–Ar), 8.37 (1H, s, OH).

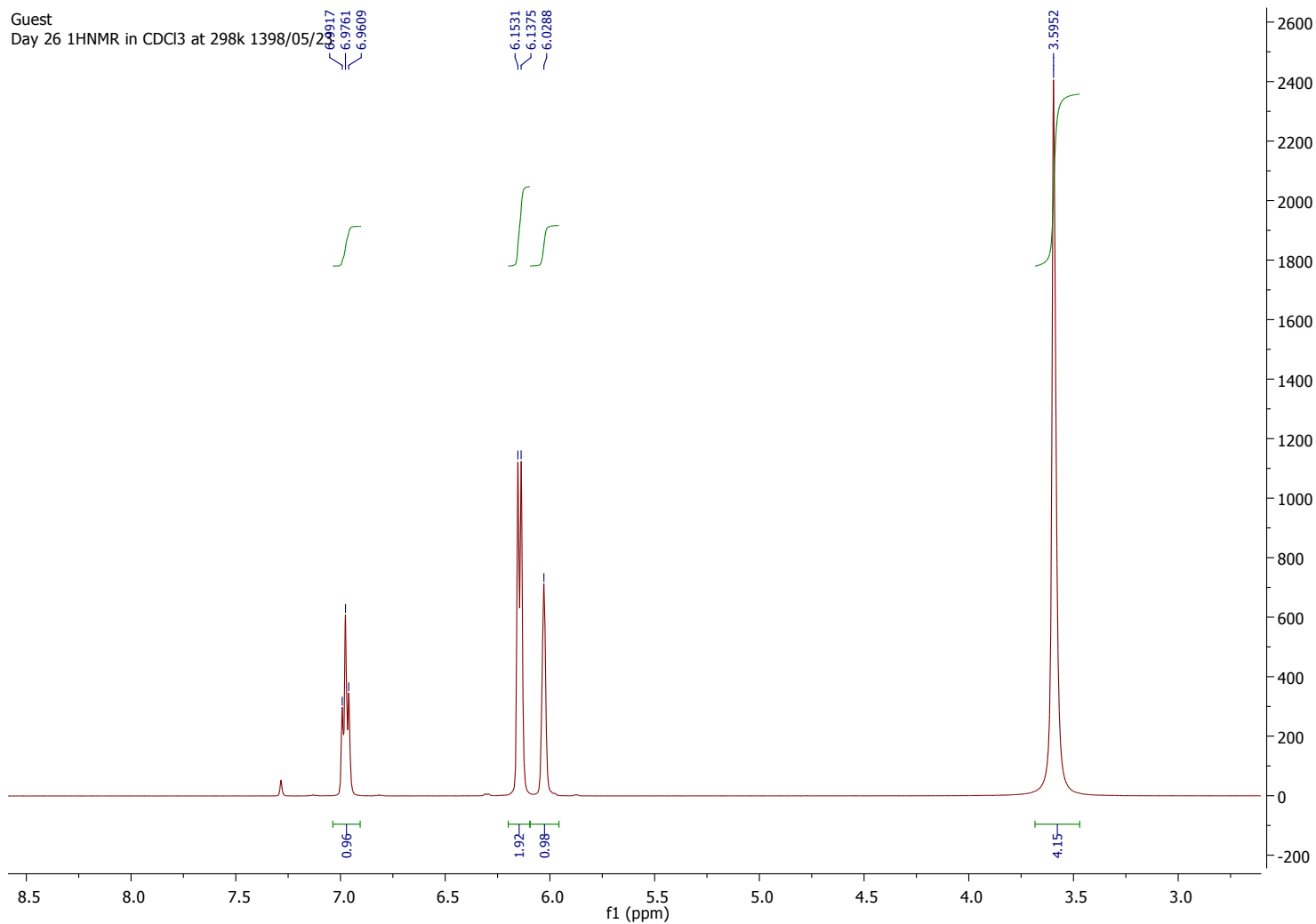
Figure S11. ¹H-NMR spectra and spectral data of 4-amino-phenol.



6. 4-amino-phenol (Table 2 – Entry 6)

^{13}C NMR (500 MHz, DMSO): δ 168.09, 153.70, 131.82, 113.18.

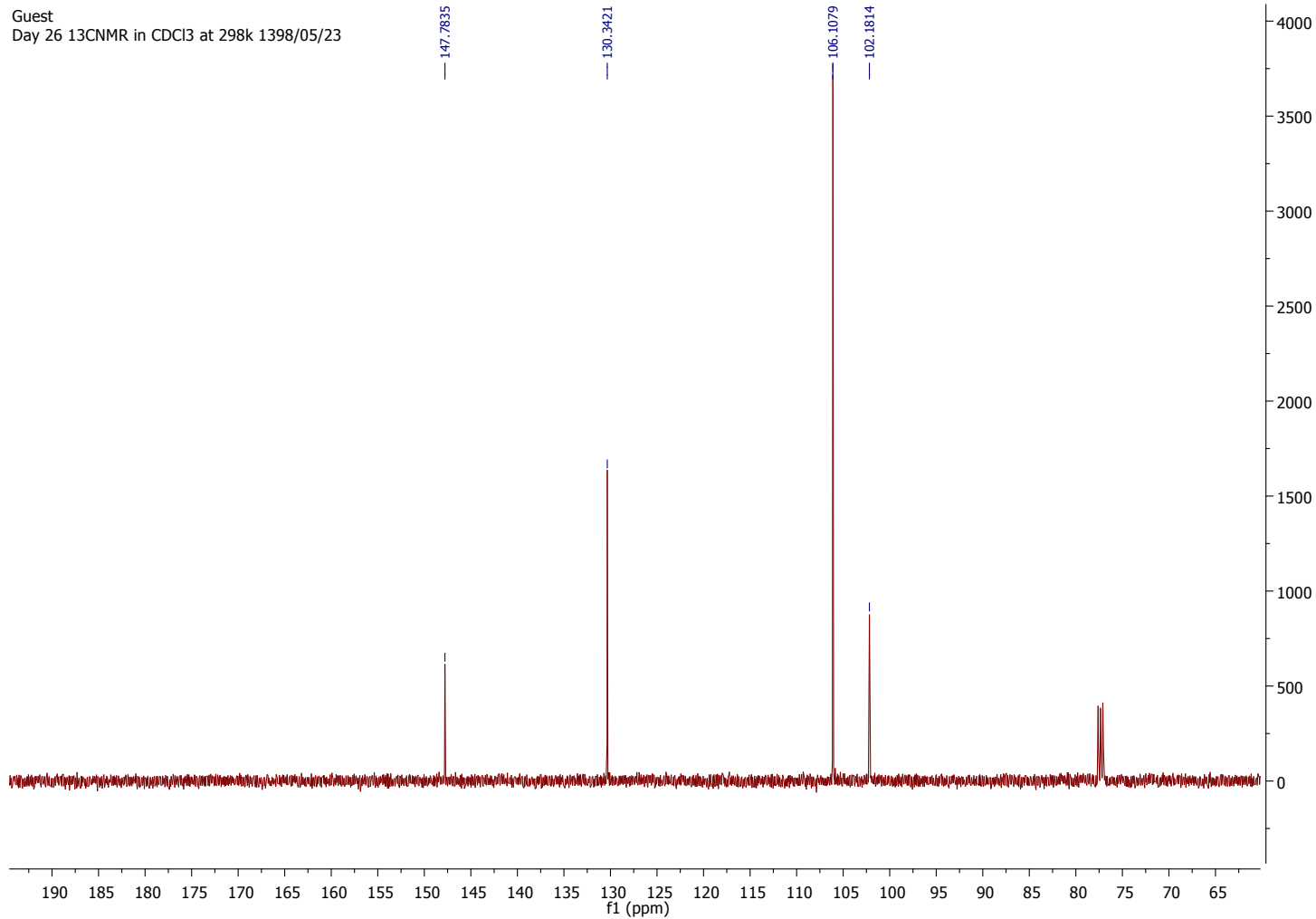
Figure S12. ^{13}C -NMR spectra and spectral data of 4-amino-phenol.



7. benzene-1,3-diamine (Table 2 – Entry 7)

¹H NMR (500 MHz, CDCl₃): δ 6.96-6.99 (m, 1 H), 6.15–6.13 (d, J = 7.8 Hz, 2 H), 6.03 (s, 1 H), 3.59 (s, 4 H).

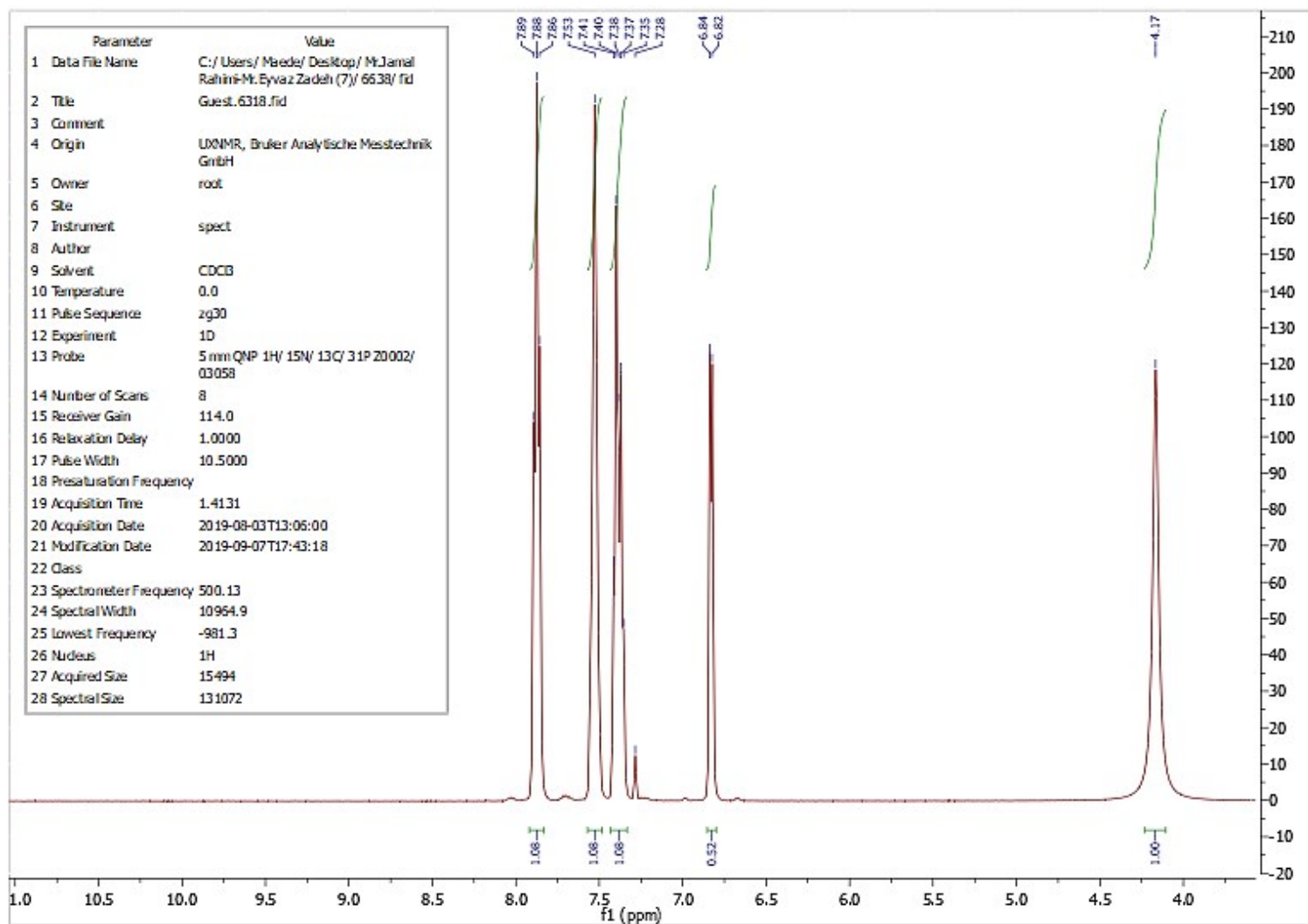
Figure S13. ¹H-NMR spectra and spectral data of benzene-1,3-diamine.



7. benzene-1,3-diamine (Table 2 – Entry 7)

^{13}C NMR (500 MHz, CDCl_3): δ 147.78, 130.34, 106.25, 102.18.

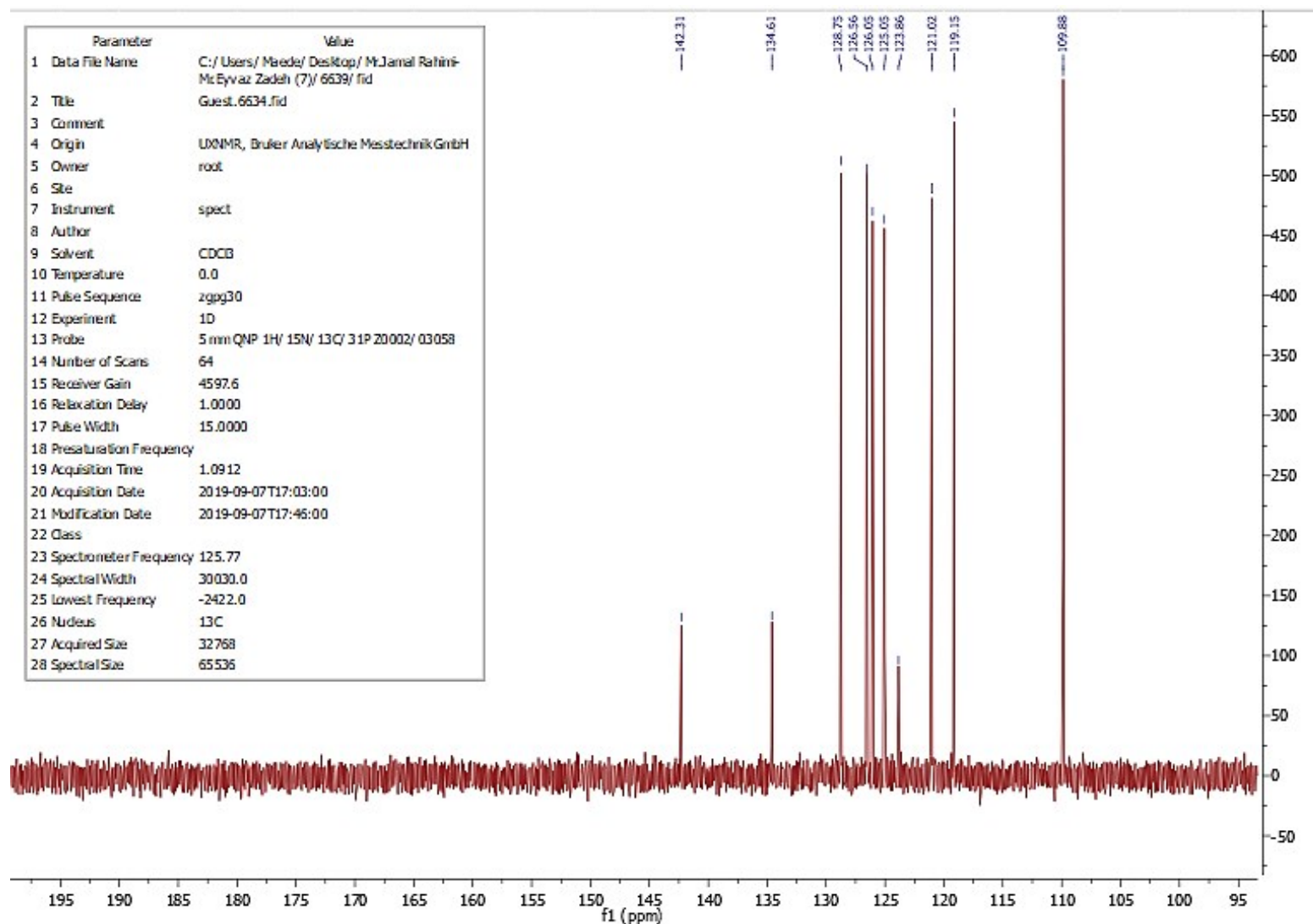
Figure S14. ^{13}C -NMR spectra and spectral data of benzene-1,3-diamine.



8. 2-Naphthylamine (Table 2 – Entry 8)

$^1\text{H-NMR}$ (500 MHz, CDCl_3): $\delta = 7.88$ (m, 2H), 7.53 (m, 2H), 7.38 (m, 2H), 6.83 (m, 1H), 4.17 (s, 2H).

Figure S15. $^1\text{H-NMR}$ spectra and spectral data of 2-Naphthylamine.

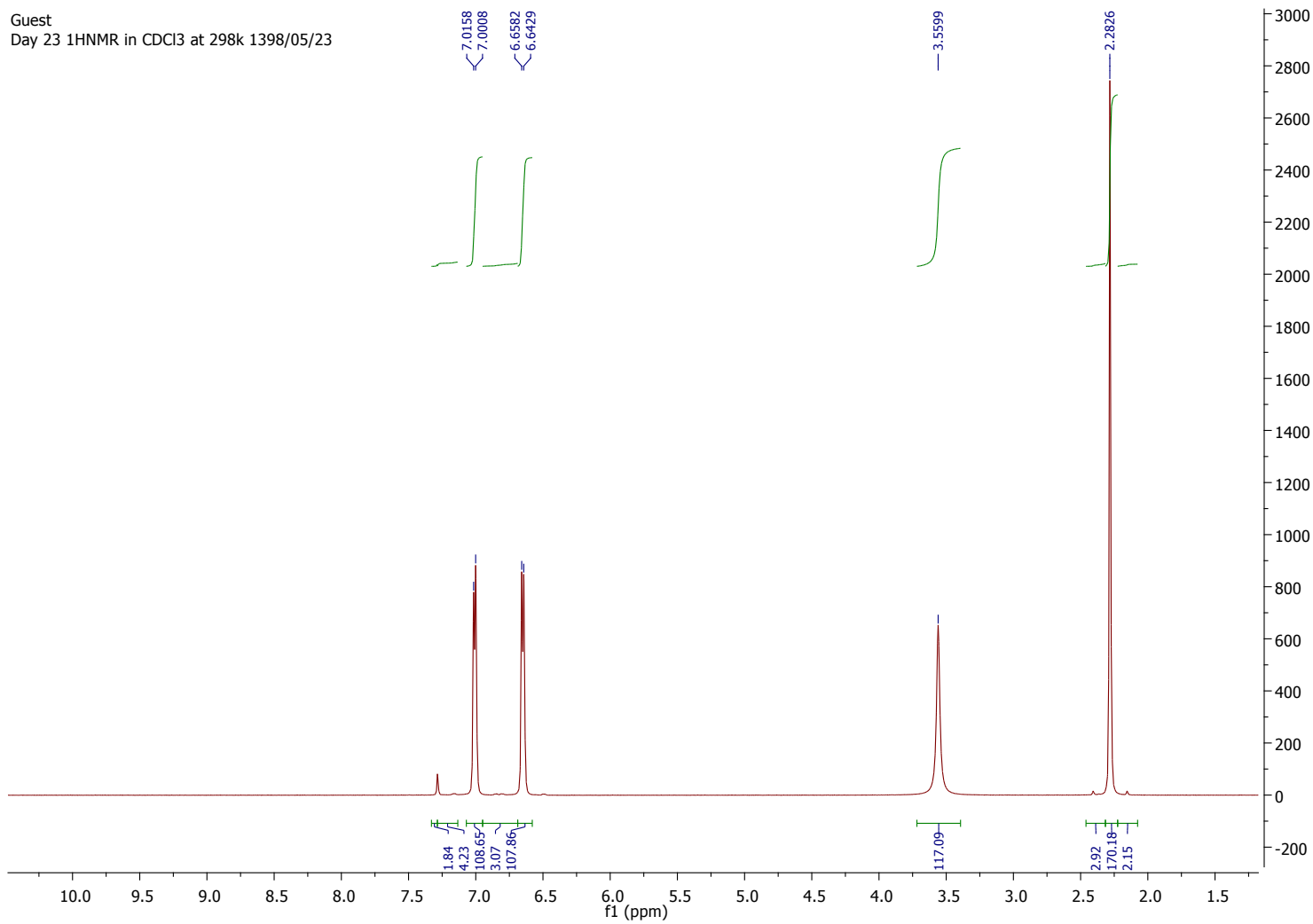


8. 2-Naphthylamine (Table 2 – Entry 8)

^{13}C -NMR (500 MHz, CDCl_3): $\delta = 142.31, 134.61, 128.75, 126.56, 126.05, 125.05, 123.86, 121.02, 119.15, 109.88$.

Figure S16. ^{13}C -NMR spectra and spectral data of 2-Naphthylamine.

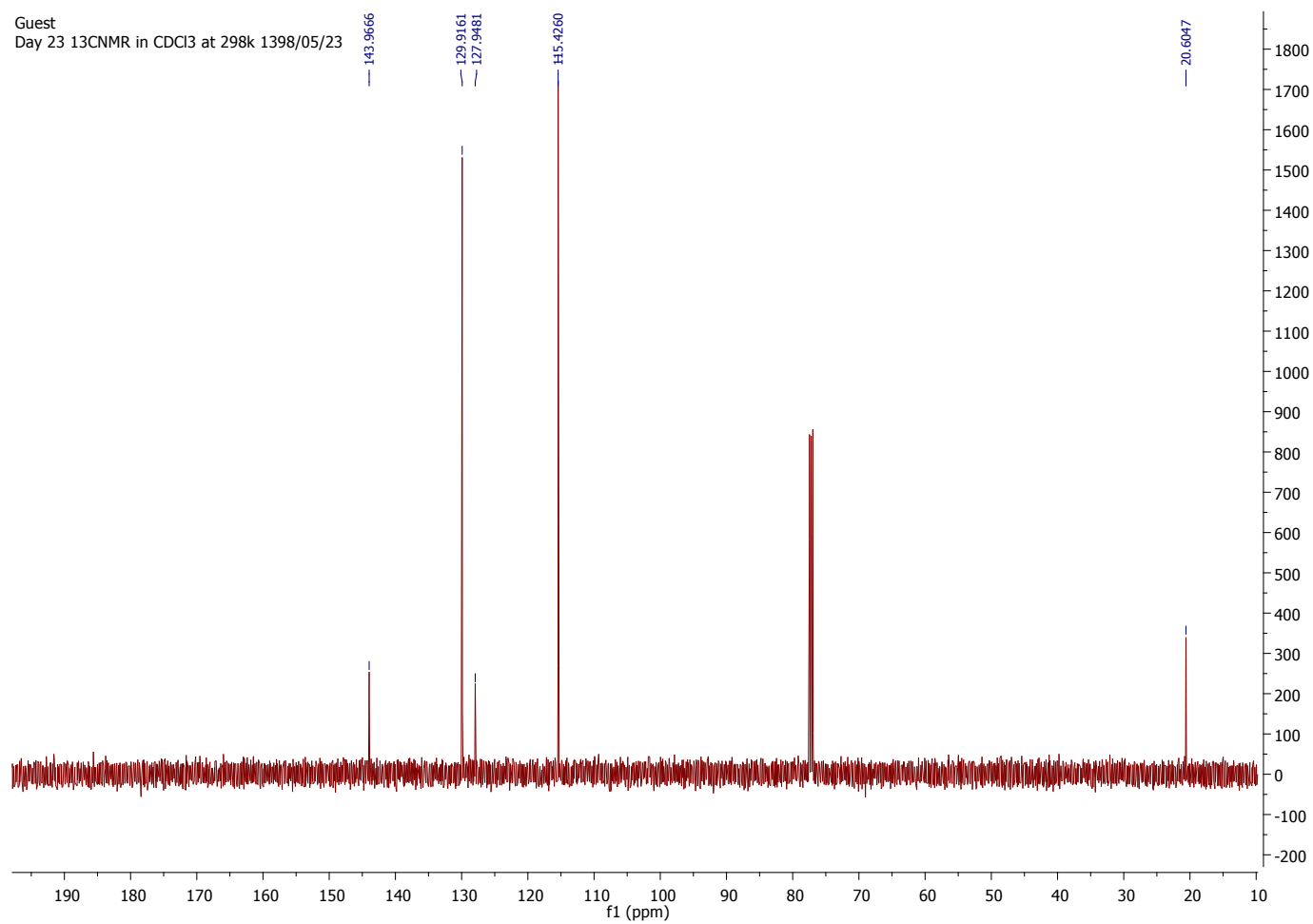
Guest
Day 23 1HNMR in CDCl3 at 298k 1398/05/23



9. p-toluidine (Table 2 – Entry 9)

¹H NMR (500 MHz, CDCl₃): δ 2.28 (s, 3H), 3.56 (s, 2H), 6.64-6.66 (d, J = 10 Hz, 2H), 7.00-7.02 (d, J = 10 Hz, 2H).

Figure S17. ¹H-NMR spectra and spectral data of p-toluidine.

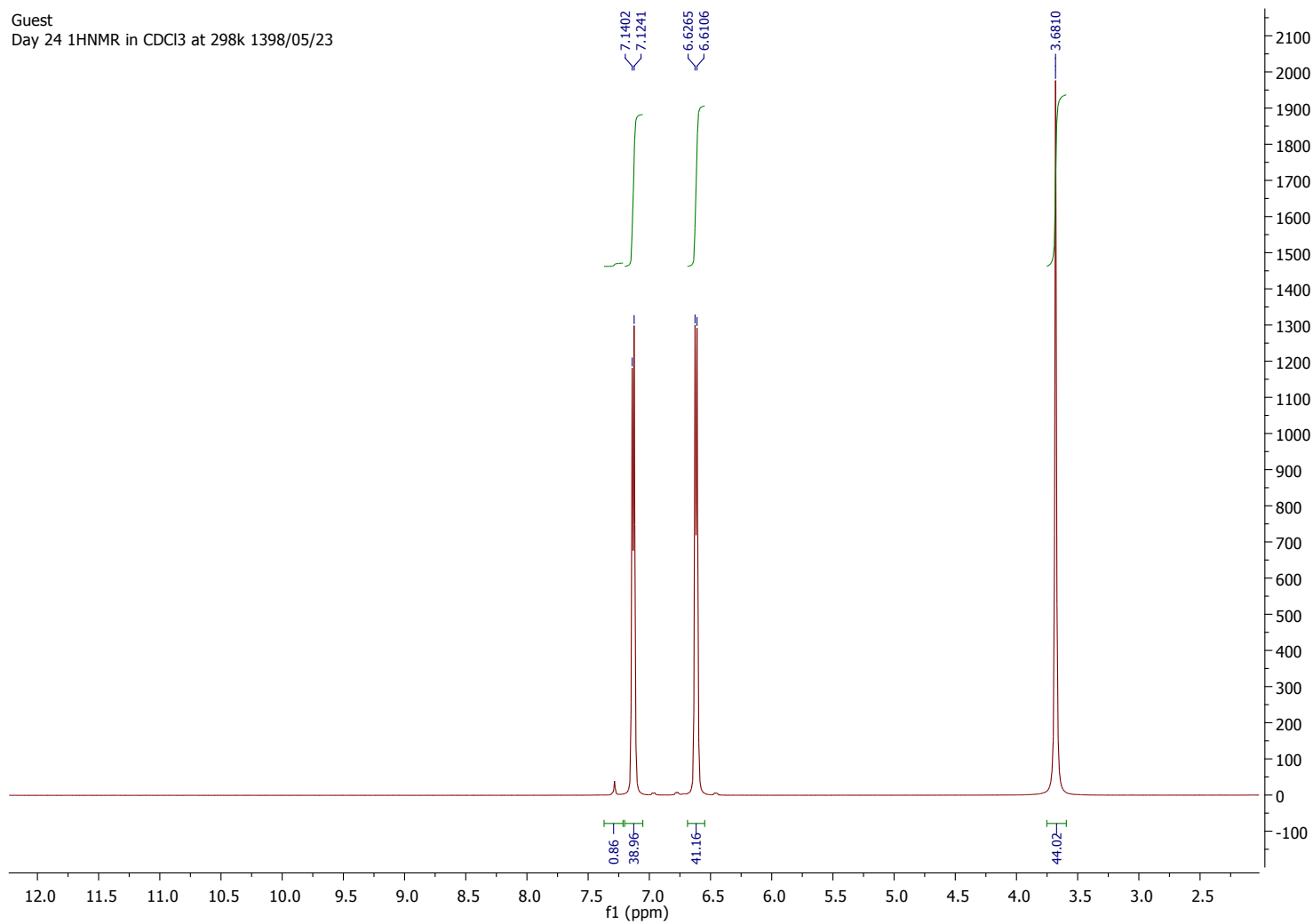


9. p-toluidine (Table 2 – Entry 9)

¹³C NMR (500 MHz, CDCl₃) δ 20.60, 115.43, 127.96, 129.92, 143.97.

Figure S18. ¹³C-NMR spectra and spectral data of p-toluidine.

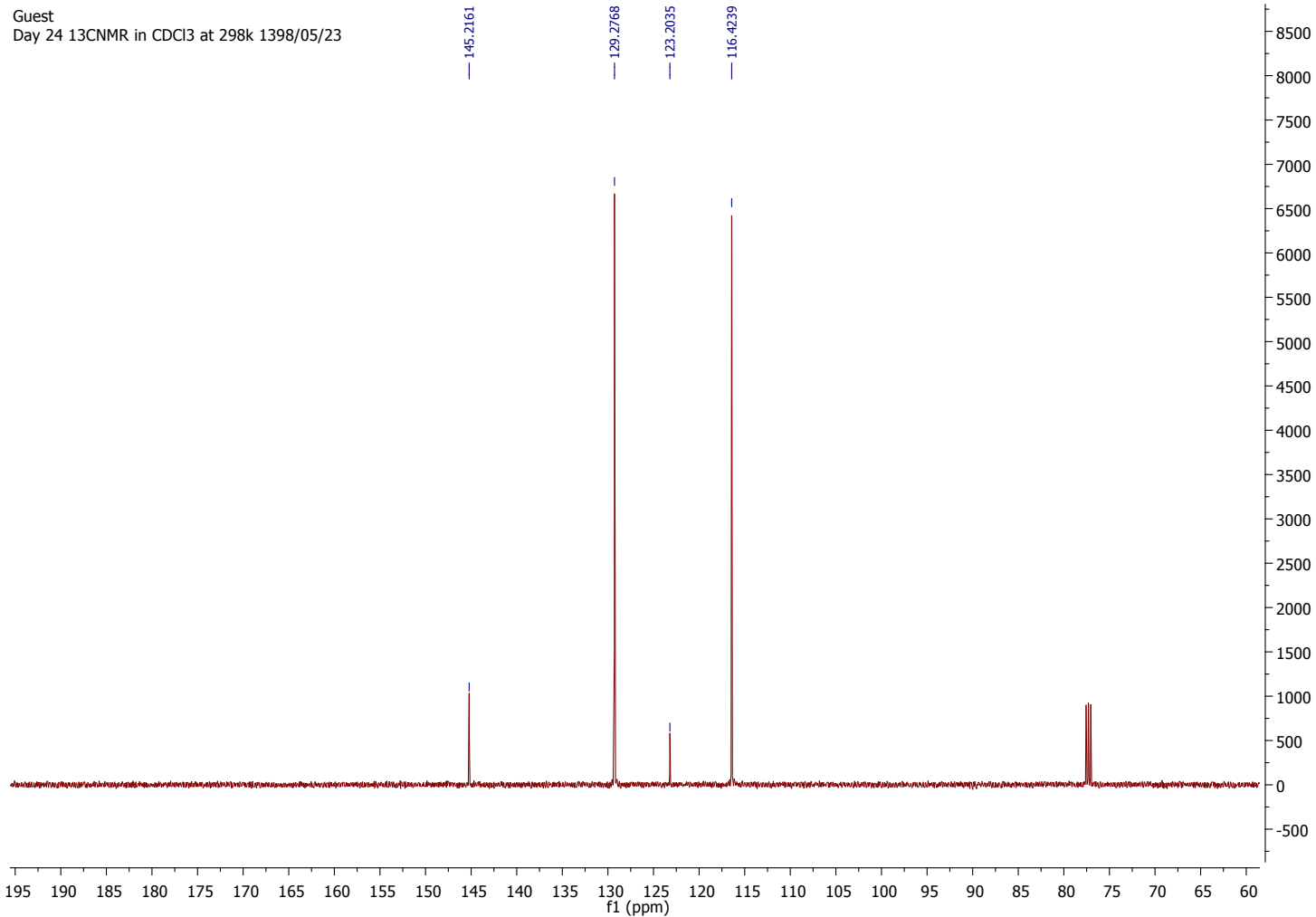
Guest
Day 24 ¹H-NMR in CDCl₃ at 298k 1398/05/23



10. 4-chloroaniline (Table 2– Entry 10)

¹H NMR (500 MHz, CDCl₃): δ 3.68 (s, 2H), 6.61-6.63 (d, J = 10 Hz, 2H), 7.12-7.14 (d, J = 10 Hz, 2H).

Figure S19. ¹H-NMR spectra and spectral data of 4-chloroaniline.



10. 4-chloroaniline (Table 2– Entry 10)

¹³C NMR (500 MHz, CDCl₃): δ 116.42, 123.20, 129.28, 145.22.

Figure S20. ¹³C-NMR spectra and spectral data of 4-chloroaniline.

Table S1. Results of ICP-OES analysis of Fe₃O₄@VPMP/CLS-Cu nanocomposite.

Element	Wavelength (nm)	LOD (mg/Kg)	RSD ^a (%)	ICP-OES (mg/g)
<i>Na</i>	588.995	1.01	9.11	2.0
<i>Fe</i>	259.940	0.0528	4.18	312.14
<i>Al</i>	167.081	0.459	12.6	26.52
<i>Ca</i>	422.673	0.263	5.43	3.06
<i>K</i>	769.896	3.12	15.6	2.24
<i>Cu</i>	324.754	0.0732	6.23	255.85

^a *n*=3.**Estimation of the catalyst amount in mmol% based on ICP-OES results**

Since, copper element is the main active catalytic site in the structure of the Fe₃O₄@VPMP/CLS-Cu nanocomposite, the weight ratio of Cu is considered for conversion to mmol% of the catalyst, as below;

Per 1000 mg of catalyst: 255.85 (mg Cu) = 0.255 (g Cu) = 4.01 (mmol Cu)

Based on Table 1 (in manuscript), 50.0 mg of Fe₃O₄@VPMP/CLS-Cu is subjected to the reaction mixture, under optimum conditions, so the mmol of Cu in 50.0 mg of Fe₃O₄@VPMP/CLS-Cu is calculated in 0.2 mmol (4.01/20).

Since, 1.0 mmol of the nitrobenzene (NB) derivatives is used for reduction;

$0.2 \text{ (mmol Cu)} / 1.0 \text{ (mmol NB)} \times 100 = \mathbf{20 \text{ mmol\%}}$ (catalyst used in NB reduction reactions)

Calculation of turnover number (TON) and turnover frequency (TOF)

As described above, copper is the main catalytic site in the structure of Fe₃O₄@VPMP/CLS-Cu for reductive conversion of the nitrobenzene derivatives. Hence, the mmol% of the copper element in the optimum conditions (Table 1, in manuscript) can be considered for the estimation of TON and TOF values, as below:

Turnover number (TON) = number of moles of reactant consumed / mole of catalyst

Turnover frequency (TOF) = TON / time of reaction (h)

$$\text{TON} = 98 / 20 = 4.9$$

$$\text{TOF} = 4.9 / 0.133 = 36.84 \text{ h}^{-1}$$

Estimation of half-life of the reduction reaction of nitrobenzene and investigation of reusability of $\text{Fe}_3\text{O}_4@\text{VPMP}/\text{CLS}-\text{Cu}$ catalytic system:

The *half-life* of the reduction reaction of nitrobenzene (NB) as the time it takes for the concentration of a reactant to fall to half of its original value, can be estimated by UV-Vis spectroscopy.

For this purpose, a control reaction containing NB (20 mg/mL) in water under catalytic conditions provided by a dispersion of $\text{Fe}_3\text{O}_4@\text{VPMP}/\text{CLS}-\text{Cu}$ particles (40 mg), NaBH_4 (62 mg), and K_2CO_3 (30 mg), was monitored in a range of time 0-8 minutes. For sampling at different times (2, 4, 6 and 8 min), the particles were magnetically collected by an external magnet and 5.0 μL of the mixture was withdrawn by a micropipette and diluted to 50 mL with water. Then, paper filtration was performed on the prepared samples and the prepared samples were studied by UV-Vis spectrophotometer in a wavelength range of 200-350 nm. Finally, the concentrations of the aniline and NB in the reaction mixture were calculated by the line equations obtained from the calibration curves (Figure S21a). As can be observed in Figure S21, considering the calibration curves of aniline and NB obtained from the standard solutions in different concentrations (panel a) and the provided UV-Vis spectra (panel b), the concentration balance between aniline and nitrobenzene UV-Vis spectroscopy has been created after **4 minutes** from the beginning of the reaction.

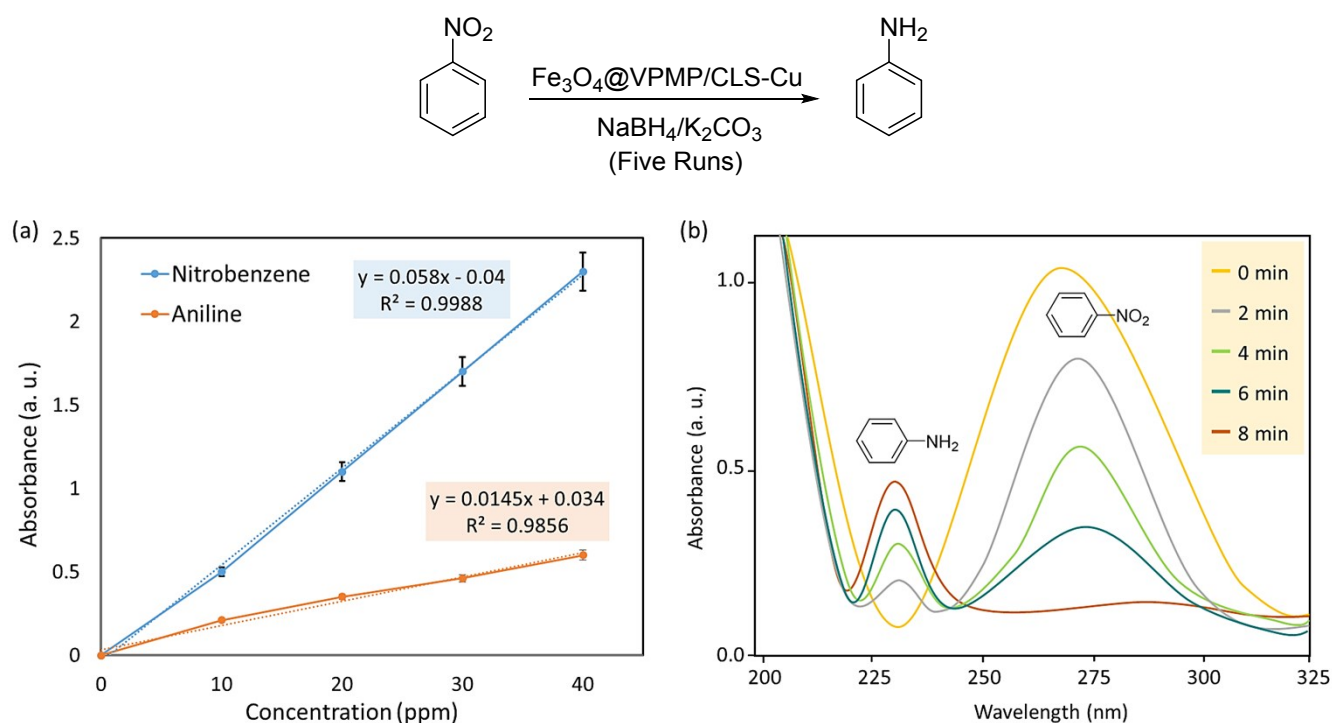


Figure S21. (a) Calibration curves of nitrobenzene (NB) and aniline solutions in different concentrations (error bars show %RSD in each point, $n = 3$), and (b) UV-Vis absorbance spectra of the NB reaction mixture, under catalytic conditions in different times.

Accordingly, the half-life values for the next successive runs in the recycling process have been estimated and reported in Table S2. As is seen in the table, the time of half-life of the reduction reaction of the NB has changed to higher values after each time of separation and re-preparation of the catalyst particles. Based on the obtained results, it can be concluded that the catalytic efficiency of the Fe₃O₄@VPMP/CLS-Cu system is gradually lost during the recycling and reusing processes. To investigate the possible reasons, probable leaching of the copper particles from the Fe₃O₄@VPMP/CLS-Cu system as the main catalytic site has been checked by inductively coupled plasma mass spectrometry (ICP-MS) analysis on the supernatant after the separation of the magnetic particles after running each recycling process. As is seen in Table S3, a bit of leaching has occurred for the copper particles during the separation, rinsing, drying and reusing of the Fe₃O₄@VPMP/CLS-Cu particles in successive five runs.

Table S2. The yields and half-life values obtained for the reduction reaction of nitrobenzene (NB), under catalytic conditions provided by Fe₃O₄@VPMP/CLS-Cu system during five times reuse.

Run	Half-life (min)	RSD ^a (%)	Reaction yield ^b (%)
1	4.0	5.0	98
2	4.3	4.8	94
3	4.5	6.6	91
4	4.6	3.7	89
5	4.8	7.1	86

^a Relative standard deviations have been estimated for three samples per each condition ($n = 3$); ^b Reaction time: 8 minute, isolated yields after purification of the aniline.

Table S3. Results of ICP-MS analysis on copper ion exist in supernatants after separation of the magnetic particles, after running each recycling process (leaching test).

Run	LOD (ppm)	RSD ^a (%)	ICP-MS (ppm)
1	0.03	2.1	9.4
2	0.03	1.1	7.6
3	0.03	1.6	4.3
4	0.03	2.3	3.8
5	0.03	1.4	3.1

^a $n=3$.

Table S4. Results of ICP-OES analysis of the recovered Fe₃O₄@VPMP/CLS-Cu nanocomposite.

Element	Wavelength (nm)	LOD (mg/Kg)	RSD ^a (%)	ICP-OES (mg/g)
<i>Na</i>	588.995	1.01	9.11	1.71
<i>Fe</i>	259.940	0.0528	4.18	299.29
<i>Al</i>	167.081	0.459	12.6	25.67
<i>Ca</i>	422.673	0.263	5.43	2.88
<i>K</i>	769.896	3.12	15.6	1.39
<i>Cu</i>	324.754	0.0732	6.23	207.12

^a *n*=3.

Optimization

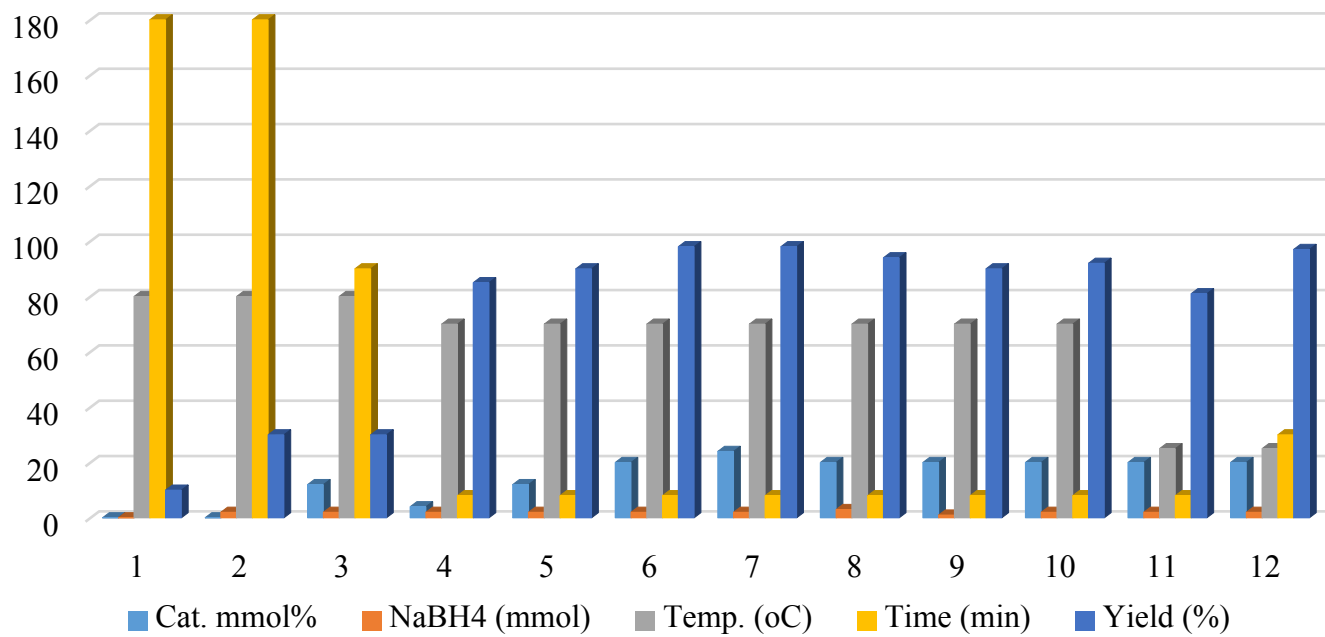


Figure S22. The graph of the optimization stages of reduction reaction of nitrobenzene under various catalytic conditions (related to Table 1).